Reactions of N(2^2D) with H_2O and D_2O; Identification of the Two Exit Channels, NH(ND) + OH(OD) and H(D) + HNO(DNO)

Hironobu Umemoto,* Takashi Asai, Hideomi Hashimoto, and Takanobu Nakae

Department of Chemical Materials Science, Japan Advanced Institute of Science and Technology,
Asahidai, Tatsunokuchi, Nomi, Ishikawa 923- 1292, Japan

Received: October 5, 1998; In Final Form: November 25, 1998

Ground-state NH(ND) and OH(OD) radicals as well as H(D) atoms were detected as products in the reaction of N(^{2}D) with $H_2O(D_2O)$. The nascent NH(v''=1)/NH(v''=0) population ratio is 0.3, while the OH(v''=1)/OH(v''=0) ratio is less than 0.05. The rotational state distributions of NH(v''=0) and OH(v''=0) can be characterized by Boltzmann distributions at 3000 and 2000 K, respectively. Similar results were obtained for ND and OD, and no large H/D isotope effect was observed in the energy distributions. Rotational excitation of not only NH(ND) but also OH(OD) suggests that these reactions are not direct but include complex formation processes. The average energy released into the translational mode in the production of H + HNO is 65 kJ mol^{-1}, which corresponds to 45% of the available energy. That for the D + DNO channel was determined to be 47%.

Introduction

In the A + BCD type reactions to produce AB + CD, the newly formed AB molecule is usually more excited than the old one, CD. For example, in the reaction of H with NO_2, OH is vibrationally and rotationally more excited than NO.[1,2] There are many other examples.[3−6] These reactions are regarded as direct ones in which long-lived intermediate complexes are not formed. On the other hand, in the reaction of O($^1D_2$) with HCN, CN is hot while OH is cool.[7] Similar behavior has also been observed in the reactions of O(^{3}P) with ND_2 and Cl with HCN.[8,9] In these reactions, the character of the intermediate complexes plays important roles.

The reaction of O($^1D_2$) with H_2O is an intermediate case. This reaction has been investigated extensively.[10−17] In this system, isotopically labeled reagent, $H_2{}^{18}O$, is used to distinguish new and old OH fragments. The new OH fragment is more energetic, both internally and translationally, than the old one. However, the excitation of old OH cannot be ignored. The geometry of the reaction intermediate has been discussed vigorously on the basis of these results. However, it is not certain, yet, if the reaction is abstractive or insertive.[15−17] It is desired to study the reaction of a similar but different system. The reaction of N(^{2}D) with H_2O should be one of such candidates.

In the reaction of O($^1D_2$) with H_2O, it has been recognized that the production of two OH radicals is the only plausible exit channel.[18] The production of HO_2 + H is endothermic under thermal conditions. On the other hand, the reaction of N(^{2}D) with H_2O has several exits, including the production of H atoms:

$$\mathrm{N(^2D) + H_2O \rightarrow NH(X\ ^3\Sigma^-) + OH(X\ ^2\Pi) + 61\ kJ\ mol^{-1}} \quad (1)$$

$$\mathrm{\rightarrow HNO(^1A') + H + 143\ kJ\ mol^{-1}} \quad (2)$$

$$\mathrm{\rightarrow HNO(^3A'') + H + 52\ kJ\ mol^{-1}} \quad (3)$$

$$\mathrm{\rightarrow HON(^3A'') + H + 26\ kJ\ mol^{-1}} \quad (4)$$

$$\mathrm{\rightarrow NO + H_2 + 369\ kJ\ mol^{-1}} \quad (5)$$

$$\mathrm{\rightarrow NH_2 + O + 26\ kJ\ mol^{-1}} \quad (6)$$

Here, the exothermicities for reactions 3 and 4 are cited from recent ab initio calculations at the PMP4(full,SDTQ)/cc-pVTZ//MP2(full)/cc-pVTZ level.[19] In the present work, we have identified NH(ND), OH(OD), and H(D). The overall rate constants for the deactivation of N(^{2}D) by H_2O and D_2O were also determined.[20]

Experimental Section

The experimental apparatus and the procedure for the production of N(^{2}D) and the detection of radical species were similar to those described elsewhere.[20−25] NO was two-photon photolyzed with the frequency-doubled output of a Nd:YAG pumped dye laser (Quanta-Ray, GCR-170/PDL-3) at 275.3 nm. The photolysis beam was focused by using a 200 mm focal-length lens.

NH(ND) and OH(OD) radicals were detected by laser-induced fluorescence. A dye laser (Lambda Physik, LPD3000E) pumped with a XeF excimer laser (Lambda Physik, LPX105i) or a Nd:YAG laser (Quanta-Ray, GCR-170) was used. The output of this laser was frequency-doubled by a KDP crystal. The wavelength was tuned to the A $^3\Pi_i$−X $^3\Sigma^-$ transition around

---

* Correponding author. E-mail: umemoto@jaist.ac.jp.

10.1021/jp9839605 CCC: $18.00 © 1999 American Chemical Society
Published on Web 01/22/1999

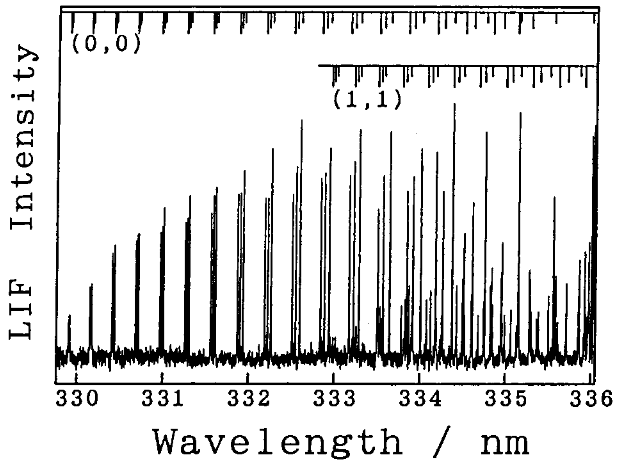

Figure 1. LIF spectrum of NH(X $^3\Sigma^-$) formed in the reaction of N(^{2}D) + H_2O. The pressures were 20 Pa for both NO and H_2O. The photolysis-probe delay time was 150 ns. The assignments are shown for the R_1, R_2, and R_3 branches of the (0,0) and (1,1) bands.

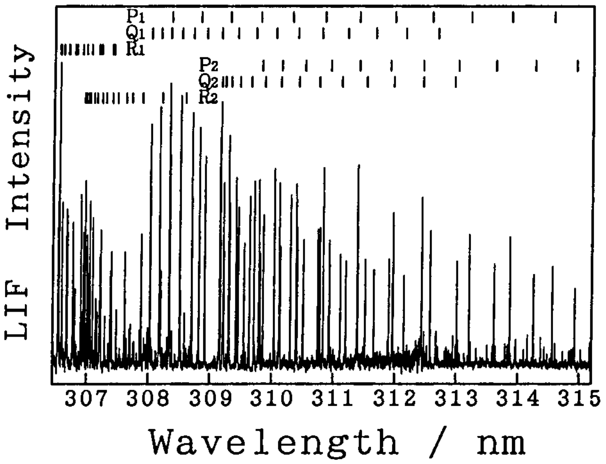

Figure 2. LIF spectrum of OH(X $^2\Pi$) formed in the reaction of N(^{2}D) + H_2O. The pressures were 14 Pa for both NO and H_2O. The photolysis-probe delay time was 150 ns. The assignments are shown for the P_1, P_2, Q_1, Q_2, R_1, and R_2 branches of the (0,0) band.

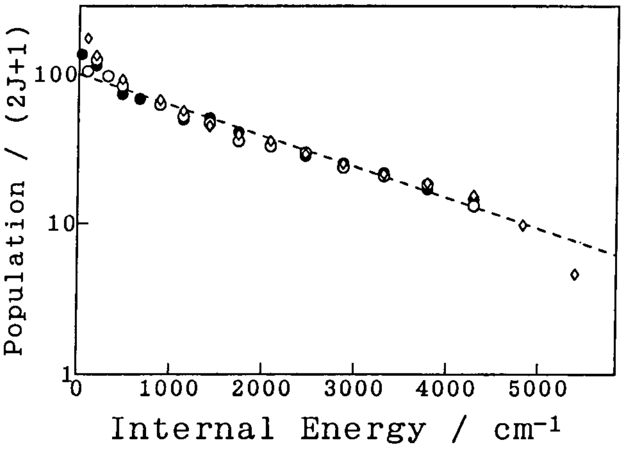

Figure 3. Boltzmann plot of relative populations of NH(X $^3\Sigma^-$, $v'' = 0$) formed in the reaction of N(^{2}D) with H_2O: R_1 (●); R_2 (○); R_3 (◇). The dotted line represents the rotational temperature of 3000 K.

336 nm for NH(ND) and to the A $^2\Sigma^+-$X $^2\Pi_i$ transition around 308 nm for OH(OD). The probe laser was weak enough, below 3 μJ/pulse, to avoid saturation. To avoid secondary relaxation processes, the delay time between the photolysis and probe pulses was kept at 150 ns, while the total pressure was kept below 40 Pa.

The detection technique of H(D) atoms was the same as that employed by Hänsch et al.[26] and has been presented elsewhere.[25] Ground-state H(D) atoms were two-photon excited to the 2^2S state. This excited state can be collisionally relaxed to the nearby 2^2P state, which fluoresces vuv light at 121.6 (121.5) nm. The vuv fluorescence was collected through an MgF_2 window (Oken, 1 mm thick) and an interference filter (Acton Research, 122-N) and detected with a solar-blind photomultiplier tube (Hamamatsu Photonics, R1459). For the two-photon excitation, the frequency-doubled output of a Nd:YAG laser (Quanta-Ray, GCR-170) pumped dye laser (Lambda Physik, LPD3000E) was employed. The typical pulse energy of the doubled output was 0.4 mJ. The bandwidth of the doubled output of the probe laser was 0.5 cm^{-1}. This laser pulse was focused into the interaction region by using a 200 mm focal-length lens. The photolysis and probe laser beams were aligned collinearly. The delay time between the photolysis and probe laser pulses was typically 50 ns, while the total pressure was 80 Pa. To avoid the diffusion of H(D) atoms from the viewing zone before they were detected, the focal points of the photolysis and probe laser beams were separated by 50 mm.

The decay profiles of N(^{2}D) concentration were measured at various H_2O(D_2O) pressures to evaluate the overall rate constant. The detection technique of N(^{2}D) is similar to that for H(D) described above. The detailed procedure has been described elsewhere.[20]

NO (Sumitomo Seika, 99.999%) was used from a cylinder without further purification. Distilled and deionized H_2O was used after being degassed under vacuum. D_2O was the product of Aldrich (isotopic purity 99.9%).

Results

A. Nascent Internal State Distributions of NH(ND) and OH(OD). Figures 1 and 2 show typical LIF spectra of NH(X $^3\Sigma^-$) and OH(X $^2\Pi$). Similar spectra were obtained for ND(X $^3\Sigma^-$) and OD(X $^2\Pi$). The populations of the rotational levels without spectral overlap can be determined by measuring the peak heights of the spectra. The detailed procedure for NH(ND) has been described in previous publications.[21-23] The spectrum assignments for OH have been given by Dieke and Crosswhite.[27] Those for OD have been reported by Clyne et al.[28] The rotational transition probabilities for the OH(A−X) system have been reported by Dimpfl and Kinsey and by Chidsey and Crosley.[29,30] The rotational transition probabilities for OD(A−X) were assumed to be the same as those for OH(A−X). It is not necessary to take into account the contribution of predissociation since only low rovibrational levels were produced in the present system.

Figures 3 and 4 show the Boltzmann plots of the relative populations of NH and OH. The dotted lines represent the rotational temperatures of 3000 and 2000 K, respectively. The rotational distributions of both NH and OH extend to their thermochemical limits. The constraint $\mathbf{j}(\mathrm{NH}) \approx -\mathbf{j}(\mathrm{OH})$ does not hold. By summing over the rotational populations, the vibrational population ratios can be determined. The ratio of NH(v''=1)/NH(v''=0) was determined to be 0.3 ± 0.1. The OH(v''=1)/OH(v''=0) ratio is less than 0.05. Production of the vibrational states over $v'' \geq 2$ is energetically inaccessible. Table 1 compares the present results with those of O($^1D_2$) + H_2O.

Very similar results were obtained for the reaction of N(^{2}D) with D_2O. The rotational temperatures of ND(v''=0) and OD(v''=0) are 3000 and 2000 K, respectively. The ND(v''=1)/ND(v''=0) ratio is 0.4 ± 0.1, while the OD(v''=1)/OD(v''=0) ratio is less than 0.05.

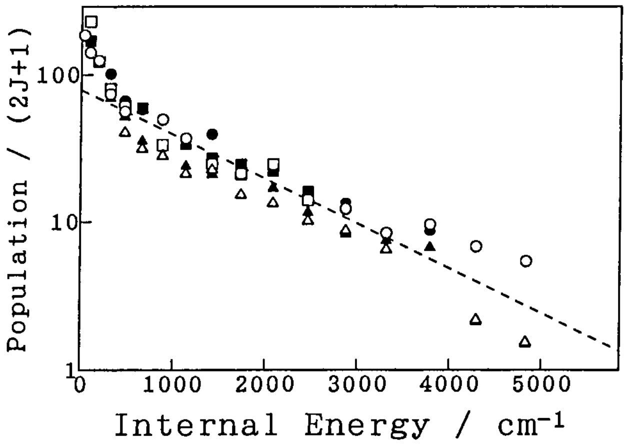

Figure 4. Boltzmann plot of relative populations of $OH(X\ ^2\Pi, v'' = 0)$ formed in the reaction of $N(^2D)$ with H_2O: P_1 (■); Q_1 (▲); R_1 (●); P_2 (□); Q_2 (△); R_2 (○). The dotted line represents the rotational temperature of 2000 K.

TABLE 1: Rotational and Vibrational Energies of NH and OH Produced in the Reactions of $N(^2D)$ and $O(^1D_2)$ with H_2O in kJ mol^{-1}

		Er- (v''=0)	Er- (v''=1)	Er[d]	Ev
$N(^2D) + H_2O$[a]	NH	19.2	10.8	17.0 (25%)	8.6 (13%)
	OH	15.9		15 (22%)	<3 (<4%)
$O(^1D) + H_2O$[b]	new OH	49.9	18.3	37.1 (22%)	>17.3 (>10%)[e]
	old OH	21.6	18.3	21.5 (13%)	1.6 (1%)
$O(^1D) + H_2O$[c]	new OH	40.7	33.3	37.6 (26%)	>18.2 (>13%)[e]
	old OH	22.4	19.1	22.3 (16%)	2.6 (2%)

[a] Available energy = 67.9 kJ mol^{-1}, this work. [b] Available energy = 165.1 kJ mol^{-1}, Tanaka et al.[17] [c] Available energy = 142.0 kJ mol^{-1}, Sauder et al.[15] [d] Weighted average of the $v'' = 0$ and $v'' = 1$ levels. [e] Production of $OH(v'' \geq 2)$ is expected, and the lower limits are shown.

OH radicals measured by probing the Q branch lines are less populated than those measured by probing the P and R transitions, although the spin states are equally populated. Similar results were obtained for OD. In other words, a preference was observed for $\Pi(A')$ over the $\Pi(A'')$ Λ doublet state. The average $\Pi(A')/\Pi(A'')$ ratio was determined to be 1.45 ± 0.20 and showed no clear dependence on the rotational quantum number, N''. It should be noted, however, that there could be some state-changing collisions under the present experimental conditions. The product of the total pressure and the pump−probe delay time, $P\Delta t$, was typically 4×10^{-6} Pa s when OH was detected. This is low enough for rotational distribution measurements.[15,22] However, more severe conditions are required when population ratios of electronic fine structures, such as those of Λ doublets, are discussed.[15] Then, the present results for the Λ doublet preference shall be treated just qualitatively.

Not only $N(^2D)$ but also $O(^1D_2)$ is produced in the two-photon dissociation of NO at 275.3 nm.[25] However, the amounts of $O(^1D_2)$ and consequently that of OH produced in the reaction of $O(^1D_2)$ with H_2O are small. The OH signal in the NO/H_2 system was measured to be less than 5% of that observed in the present NO/H_2O system when the partial pressures were set equal. Direct photolysis of H_2O at 275.3 nm to produce OH and H is negligible.

B. Translational Energy Release in the HNO(DNO) + H(D) Process. Figure 5 shows the Doppler spectrum of H atoms formed in the reaction of $N(^2D)$ with H_2O. A similar result was obtained for D_2O. Background signals of H(D) atoms appeared even in the absence of photolysis laser light. This should be ascribed to the two-photon dissociation by the probe laser. This contribution was subtracted in the figure. Measured Doppler profiles showed no change under various experimental conditions, as for the $N(^2D)/CH_4$ system.[25]

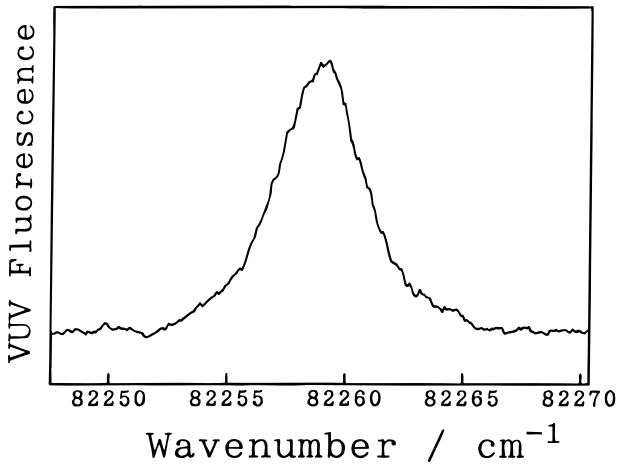

Figure 5. Doppler profile of H atoms formed in the reaction of $N(^2D)$ with H_2O. The pressures were 53 Pa for NO and 27 Pa for H_2O. The photolysis-probe delay time was 50 ns.

It is possible to evaluate the energy released into the translational mode in the center of mass frame by analyzing such spectra. The average translational energy for the $N(^2D)/H_2O$ system is 65 ± 7 kJ mol^{-1}. The translational energy released in the $N(^2D)/D_2O$ system was measured to be 67 ± 8 kJ mol^{-1}, showing no H/D isotope effect. These values are consistent with only reaction 2, the production of $HNO(^1A')$ and H. The exothermicities for reactions 3 and 4, the production of triplet state HNO or HON, are too small to account for this translational energy release. The translational energy obtained above is larger than the statistically expected value: 46.4 kJ mol^{-1}. In the calculation of the statistical translational energy, the available energy was assumed to be partitioned into all the degrees of freedom in proportion to its statistical weight. No entrance or exit barrier was assumed. The vibrational frequencies of HNO employed were 3596, 1562, and 1110 cm^{-1}.[31] Two-photon dissociation of NO at 275.3 nm is 11.7 kJ mol^{-1} exothermic. The translational energy of $N(^2D)$ in the center-of-mass frame should be 6.2 kJ mol^{-1}. The above energy is less than the thermal energy at 300 K and much smaller than the exothermicity for the reaction to produce H and HNO, 143 kJ mol^{-1}. Then, the contribution of this translational energy was ignored.

An attempt was made to detect HNO(DNO) by LIF around 618 nm,[32] but no signal could be observed. This is consistent with the low yield of H(D).

C. Absolute Yields of H and D. The absolute yield for the production of H in the reaction of $N(^2D)$ with H_2O, ϕ (H_2O), was determined by comparing the vuv fluorescence signal intensities of H over D for two mixtures, H_2O(27Pa)/D_2(27Pa)/NO(40Pa) and H_2(27Pa)/D_2(27Pa)/NO(40Pa) under single collision conditions. Using the D atom signal intensity as a reference, the signal ratio is given by the H atom production yields, $\phi(H_2)$ and $\phi(H_2O)$, and the rate constants for the overall deactivation, k_{H_2} and k_{H_2O}. Here, it is necessary to include a correction for the production of H in the reaction of $O(^1D_2)$ with H_2.[25] The yield of $O(^1D_2)$ in the dissociation of NO is estimated to be 0.5% of that of $N(^2D)$.[25] The rate constant for the deactivation of $O(^1D_2)$ by H_2 is 45 times larger than that of $N(^2D)$.[20,33,34] Then, the amount of H produced in the reaction of $O(^1D_2)$ with H_2 is estimated to be 23% of that formed in the

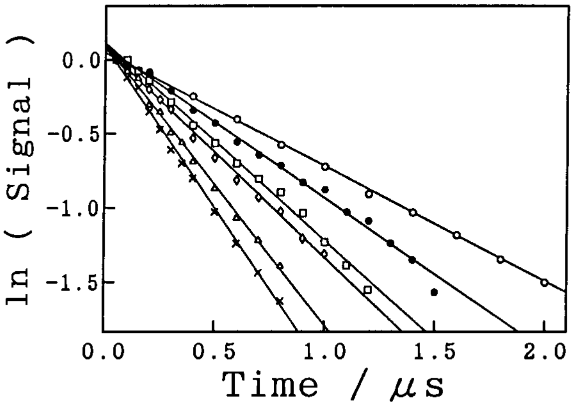

Figure 6. Semilogarithmic plots of the decay of N(^{2}D) concentration in the presence of NO and H_2O. NO pressure was 27 Pa, while H_2O pressures were 0 (○), 27 (●), 53 (□), 67 (◇), 107 (△), and 133 (×) Pa.

reaction of N(^{2}D). The experimentally obtained signal ratio, 1.7 ± 0.1, should be given by the following equation:[25]

$$\frac{([H]/[D])_{H_2O}}{([H]/[D])_{H_2}} = \frac{k_{H_2O}[H_2O]}{k_{H_2}[H_2]} \frac{\phi(H_2O)}{\phi(H_2)1.23}$$

It is not necessary to take into account the production of H in the reaction of O($^1D_2$) with H_2O because O($^1D_2$) produced in the present system does not have enough translational energy to overcome the endothermicity. The rate constants for the overall deactivation, k_{H_2} and k_{H_2O}, are 2.28×10^{-12} cm^3 s^{-1} and 4.17×10^{-11} cm^3 s^{-1}, respectively. The details for the rate constant determination shall be given in the next section. The value of $\phi(H_2)$ should be unity.[34] Then, $\phi(H_2O)$ is determined to be 0.11 ± 0.03. The error limit includes the uncertainty in the estimation of the O($^1D_2$) yield in the two-photon dissociation of NO. The absolute yield for the production of D in the reaction of N(^{2}D) with D_2O was determined similarly to be 0.17 ± 0.04.

It was difficult to determine the absolute yield of NH quantitatively. In principle, this yield can be determined by comparing the LIF signal intensities for H_2O and H_2. However, the signal intensity ratio depended on the partial pressures of H_2O and H_2. An addition reaction of NH(X $^3\Sigma^-$) to H_2O may not be ignored under long-delay conditions.

D. Rate Constant for the Deactivation of N(^{2}D). The rate constants for the deactivation of N(^{2}D) were determined under pseudo-first-order conditions. NO pressure was kept constant at 27 Pa, while H_2O(D_2O) pressure was changed between 0 and 133 Pa. To reduce the diffusional loss of N(^{2}D), 2.7 kPa of Ar was added as a buffer gas. The N(^{2}D) concentration decreased exponentially against time. Typical results for H_2O are shown in Figure 6. The decay rate increased linearly with the increase in the H_2O(D_2O) pressure. It is possible to evaluate the absolute rate constants by measuring this pressure dependence. The rate constants for H_2O and D_2O are 4.17 and 2.93×10^{-11} cm^3 s^{-1}, respectively. Those for H_2 and D_2 are 2.28 and 1.37×10^{-12} cm^3 s^{-1}, respectively.[20]

Discussion

The newly formed NH fragment has more internal energy than OH, both rotationally and vibrationally. This suggests that the complex is not sufficiently long-lived to permit complete energy randomization among all the degrees of freedom. However, OH is not a spectator. As Table 1 shows, the available energy is partitioned more evenly in the N(^{2}D)/H_2O system than in the O($^1D_2$)/H_2O system. The intermediate complex for the N(^{2}D)/H_2O system may last for a few vibrational periods, allowing some partial energy transfer or isomerization. In the reaction of Zn(4^1P_1) with H_2O,[6] it has been proposed that the production process of ZnH and OH is abstractive, because no internal excitation takes place for OH. Only ZnH is excited. The reaction of N(^{2}D) with H_2O is not such a direct one.

According to very recent ab initio molecular orbital calculations, the initial step is the addition of N(^{2}D) to the O atom of H_2O.[19] Since H_2O has an unshared electron pair, the additive H_2ON complex must be stable. During the lifetime, an H atom migrates to produce an HNOH complex. Rotational excitation of not only NH but also OH results from the moderately anisotropic decomposition of a bent *cis*- or *trans*-HNOH intermediate. The inefficient vibrational excitation of OH suggests that the O−H bond distance of the intermediate complex is similar to that of free OH. A similar mechanism may also be possible in the reaction of O($^1D_2$) with H_2O. Zn(4^1P_1) may also attack the O atom of H_2O, but the main exit, in this case, should be the production of ZnOH and H.[6]

As for Λ doublet preference in OH radicals, $\Pi(A')$ is more populated than $\Pi(A'')$. This is similar to that observed in the O($^1D_2$) + H_2O system.[14,15,17] It should be noted that the preferential production of Π (A′) is very common in the reactions of O($^1D_2$).[14,15,17,35−40] The preferential production of $\Pi(A'')$ has never been reported. The preferential production of $\Pi(A')$ is consistent with the “unconstrained dynamics prior” model.[41] This model is just statistical and the $\Pi(A')/\Pi(A'')$ ratio is predicted to be 2:1 at the high *N* limit. It is doubtful if the present observed Λ preference reflects any dynamics, because the present reaction is not a direct one.

The rate constants for the overall deactivation by H_2O and D_2O are much larger than those by CH_4 and H_2[20,42] but still smaller than the gas kinetic one. H_2O is 1.4 times more reactive than D_2O. This isotope effect is similar to that observed between CH_4 and CD_4.[20,42] In the reactions with CH_4 and CD_4, the presence of activation barriers has been demonstrated.[42] The rate constants smaller than the gas kinetic one as well as the isotope effect between H_2O and D_2O may suggest the presence of small activation barriers. However, this is not the only explanation. N(^{2}D) is 5-fold degenerate when the spin−orbit interaction is not taken into account. According to the recent molecular orbital calculations, only the lowest spin−orbit state of the N(^{2}D)/H_2O system leads to the reaction.[19] The small rate constant can be explained by the inefficient nonadiabatic transition among the five spin−orbit states. The isotope effect may result from the difference in the vibrational partition functions.

The translational energy release in the H + HNO production process is 19 kJ mol^{-1} larger than the statistically expected one. This suggests the presence of an exit barrier. There are two possible paths for the production of H and HNO. One is the O−H bond cleavage from HNOH. Another is the N−H bond cleavage from H_2NO. In both cases, H atom migration is necessary. During the migration, the excess energy must also disperse. The nonstatistical translational energy release may not be caused by the insufficient energy dispersion. Ab initio calculations also support the presence of exit barriers. The calculated barrier height to produce H + HNO from *trans*-HNOH is 53 kJ mol^{-1}, while that from H_2NO is 26 kJ mol^{-1} at the PMP4(full,SDTQ)/cc-pVTZ//MP2(full)/cc-pVTZ level.[19]

The yield for the production of H atoms in the present N(^{2}D)/H_2O system is much smaller than that in the N(^{2}D)/CH_4 system, 0.8 ± 0.2.[25] The presence of an exit barrier can be a cause of this small yield. In addition, the difference in exothermicity may contribute to this difference. In the reaction with CH_4, the production of H is 190 kJ mol^{-1} more exothermic than the production of NH, while that is only 83 kJ mol^{-1} more exothermic in the reaction with H_2O. The production of H_2 and NO is the most exothermic in the $N(^2D)/H_2O$ system, but this may not be a preferred channel because this reaction is three-centered and requires a high activation energy.[19] Similar molecular elimination processes are also minor in the $O(^1D_2)$ reactions.[18,33,43,44]

Conclusions

H_2O deactivates $N(^2D)$ efficiently, although the rate is less than gas kinetic. The production of $NH(^3\Sigma^-) + OH(^2\Pi)$ is one of the main exit channels. The H + $HNO(^1A')$ channel was also identified but cannot be major. The internal state distributions of NH and OH are nonstatistical, suggesting that the intermediate complex is not sufficiently long-lived to permit complete energy randomization. However, the available energy is partitioned not only into the internal mode of NH but also into that of OH. Since H_2O has an unshared electron pair, the additive H_2ON complex must be stable. During the lifetime, an H atom migrates to produce an HNOH complex, which decomposes to NH + OH or H + HNO. The average translational energy release in the H + HNO channel is larger than the statistically expected one. There must be an exit barrier. Similar results were obtained for D_2O. No H/D isotope effect was observed in the internal as well as translational energy distributions. Quantum effects such as tunneling do not play any important roles.

Acknowledgment. This work was partially defrayed by the Grant for Basic Science Research Projects of the Sumitomo Foundation. This study was also supported by the REIMEI Research Resources of Japan Atomic Energy Research Institute. The authors are grateful to Dr. Toshiyuki Takayanagi and Dr. Yuzuru Kurosaki of Japan Atomic Energy Research Institute for valuable discussions.

References and Notes

(1) Irvine, A. M. L.; Smith, I. W. M.; Tuckett, R. P.; Yang, X.-F. *J. Chem. Phys.* **1990**, *93*, 3177.

(2) Irvine, A. M. L.; Smith, I. W. M.; Tuckett, R. P. *J. Chem. Phys.* **1990**, *93*, 3187.

(3) Honma, K.; Fujimura, Y.; Kajimoto, O.; Inoue, G. *J. Chem. Phys.* **1988**, *88*, 4739.

(4) de Juan, J.; Callister, S.; Reisler, H.; Segal, G. A.; Wittig, C. *J. Chem. Phys.* **1988**, *89*, 1977.

(5) Adelman, D. E.; Filseth, S. V.; Zare, R. N. *J. Chem. Phys.* **1993**, *98*, 4636.

(6) Kuwahara, K.; Ikeda, H.; Umemoto, H.; Sato, T.; Takano, K.; Tsunashima, S.; Misaizu, F.; Fuke, K. *J. Chem. Phys.* **1993**, *99*, 2715.

(7) Kreher, C.; Theinl, R.; Gericke, K.-H. *J. Chem. Phys.* **1995**, *103*, 8901.

(8) Patel-Misra, D.; Sauder, D. G.; Dagdigian, P. J. *J. Chem. Phys.* **1991**, *95*, 955.

(9) Metz, R. B.; Pfeiffer, J. M.; Thoemke, J. D.; Crim, F. F. *Chem. Phys. Lett.* **1994**, *221*, 347.

(10) Gericke, K.-H.; Comes, F. J.; Levine, R. D. *J. Chem. Phys.* **1981**, *74*, 6106.

(11) Comes, F. J.; Gericke, K.-H.; Manz, J. *J. Chem. Phys.* **1981**, *75*, 2853.

(12) Butler, J. E.; Talley, L. D.; Smith, G. K.; Lin, M. C. *J. Chem. Phys.* **1981**, *74*, 4501.

(13) Guillory, W. A.; Gericke, K.-H.; Comes, F. J. *J. Chem. Phys.* **1983**, *78*, 5993.

(14) Cleveland, C. B.; Wiesenfeld, J. R. *J. Chem. Phys.* **1992**, *96*, 248.

(15) Sauder, D. G.; Stephenson, J. C.; King, D. S.; Casassa, M. P. *J. Chem. Phys.* **1992**, *97*, 952.

(16) King, D. S.; Sauder, D. G.; Casassa, M. P. *J. Chem. Phys.* **1992**, *97*, 5919.

(17) Tanaka, N.; Takayanagi, M.; Hanazaki, I. *Chem. Phys. Lett.* **1996**, *254*, 40.

(18) Zellner, R.; Wagner, G.; Himme, B. *J. Phys. Chem.* **1980**, *84*, 3196.

(19) Kurosaki, Y.; Takayanagi, T. *J. Phys. Chem. A*, in press.

(20) Umemoto, H.; Hachiya, N.; Matsunaga, E.; Suda, A.; Kawasaki, M. *Chem. Phys. Lett.* **1998**, *296*, 203.

(21) Umemoto, H.; Kimura, Y.; Asai, T. *Chem. Phys. Lett.* **1997**, *264*, 215.

(22) Umemoto, H.; Asai, T.; Kimura, Y. *J. Chem. Phys.* **1997**, *106*, 4985.

(23) Umemoto, H.; Kimura, Y.; Asai, T. *Bull. Chem. Soc. Jpn.* **1997**, *70*, 2951.

(24) Umemoto, H. *Chem. Phys. Lett.* **1998**, *292*, 594.

(25) Umemoto, H.; Nakae, T.; Hashimoto, H.; Kongo, K.; Kawasaki, M. *J. Chem. Phys.* **1998**, *109*, 5844.

(26) Hänsch, T. W.; Lee, S. A.; Wallenstein, R.; Wieman, C. *Phys. Rev. Lett.* **1975**, *34*, 307.

(27) Dieke, G. H.; Crosswhite, H. M. *J. Quantitative Spectrosc. Radiat. Trans.* **1962**, *2*, 97.

(28) Clyne, M. A. A.; Coxon, J. A.; Woon Fat, A. R. *J. Mol. Spectrosc.* **1973**, *46*, 146.

(29) Dimpfl, W. L.; Kinsey, J. L. *J. Quantitative Spectrosc. Radiat. Trans.* **1979**, *21*, 233.

(30) Chidsey, I. L.; Crosley, D. R. *J. Quantitative Spectrosc. Radiat. Trans.* **1980**, *23*, 187.

(31) Herzberg, G. *Molecular Spectra and Molecular Structure III. Electronic Spectra and Electronic Structure of Polyatomic Molecules*; Van Nostrand Reinhold: Princeton, NJ, 1967.

(32) Dixon, R. N.; Noble, M.; Taylor, C. A.; Delhoume, M. *Faraday Discuss. Chem. Soc.* **1981**, *71*, 125.

(33) Matsumi, Y.; Tonokura, K.; Inagaki, Y.; Kawasaki, M. *J. Phys. Chem.* **1993**, *97*, 6816.

(34) Suzuki, T.; Shihira, Y.; Sato, T.; Umemoto, H.; Tsunashima, S. *J. Chem. Soc., Faraday Trans.* **1993**, *89*, 995.

(35) Butler, J. E.; Jursich, G. M.; Watson, I. A.; Wiesenfeld, J. R. *J. Chem. Phys.* **1986**, *84*, 5365.

(36) Cleveland, C. B.; Jursich, G. M.; Trolier, M.; Wiesenfeld, J. R. *J. Chem. Phys.* **1987**, *86*, 3253.

(37) Park, C. R.; Wiesenfeld, J. R. *J. Chem. Phys.* **1991**, *95*, 8166.

(38) Córdova, J. F.; Rettner, C. T.; Kinsey, J. L. *J. Chem. Phys.* **1981**, *75*, 2742.

(39) Honma, K. *J. Chem. Phys.* **1993**, *99*, 7677.

(40) Wada, S.; Obi, K. *J. Phys. Chem. A* **1998**, *102*, 3481.

(41) Bronikowski, M. J.; Zare, R. N. *Chem. Phys. Lett.* **1990**, *166*, 5.

(42) Takayanagi, T.; Kurosaki, Y.; Sato, K.; Misawa, K.; Kobayashi, Y.; Tsunashima, S. *J. Phys. Chem. A*, in press.

(43) Hack, W.; Thiesemann, H. *J. Phys. Chem.* **1995**, *99*, 17364.

(44) Sanders, N. D.; Butler, J. E.; McDonald, J. R. *J. Chem. Phys.* **1980**, *73*, 5381.